ACS Chemical Neuroscience

Article

Computationally Guided Identification of Allosteric Agonists of the Metabotropic Glutamate 7 Receptor

José María Cid, Hilde Lavreysen, Gary Tresadern, Laura Pérez-Benito, Fulgencio Tovar, Alberto Fontana, and Andrés A. Trabanco

ACS Chem. Neurosci., **Just Accepted Manuscript** • DOI: 10.1021/acschemneuro.8b00331 • Publication Date (Web): 14 Sep 2018

ACS Publications

is published by the American Chemical Society. 1155 Sixteenth Street N.W., Washington, DC 20036

Computationally Guided Identification of Allosteric Agonists of the Metabotropic Glutamate 7 Receptor

Jose María Cid,[1,] Hilde Lavreysen,[2] Gary Tresadern,[2] Laura Pérez-Benito,[3] Fulgencio Tovar,[4] Alberto Fontana[1] and Andrés A. Trabanco[1,*]*

[1] Janssen Research and Development, Calle Jarama 75A, Toledo, 45007, Spain. [2]Janssen Research and Development, Turnhoutseweg 30, 2440, Beerse, Belgium. [3]Laboratori de Medicina Computacional Unitat de Bioestadistica, Facultat de Medicina, Universitat Autonoma de Barcelona, Spain. [4]Villapharma Research S.L., Parque Tecnológico de Fuente Álamo. Ctra. El Estrecho-Lobosillo, Km. 2.5- Av. Azul 30320 Fuente Álamo de Murcia, Murcia, Spain.

[*]Corresponding Authors. (J.M.C.) Tel.: +34 925 245750. E-mail: jcid@its.jnj.com; (A.A.T.) Tel.: +34 925 245750. E-mail: atrabanc@its.jnj.com

ABSTRACT

The metabotropic glutamate 7 ($mGlu_7$) receptor belongs to the group III of mGlu receptors. Since the $mGlu_7$ receptor can control excitatory neurotransmission in the hippocampus and cortex, modulation of the receptor may has therapeutic benefit in several CNS diseases. However, $mGlu_7$ remains relatively unexplored amongst the eight known mGlu receptors partly because of the limited availability of tool compounds to interrogate its potential therapeutic utility. Here we report the discovery of a new class of $mGlu_7$ allosteric agonists. Hits originating from virtual screening were followed up with further analogue searching and screening leading to a novel series of $mGlu_7$ allosteric agonists. Guided by docking into a structural model of the $mGlu_7$ receptor the initial hit **5** was successfully optimized to analogues with comparable potencies and more attractive drug-like attributes than AMN082.

KEYWORDS: $mGlu_7$, metabotropic, glutamate, allosteric, PAM, virtual screening, homology model.

INTRODUCTION

The metabotropic glutamate 7 ($mGlu_7$) receptor is a class C GPCR and belongs to the subfamily group III of metabotropic glutamate (mGlu) receptors along with $mGlu_4$, $mGlu_6$ and $mGlu_8$. The $mGlu_7$ receptor is widely distributed in the central nervous system (CNS)[1,2,3,4,5,6].It is preferentially and specifically enriched on excitatory terminals that contact inhibitory interneurons in the hippocampus and cortex. It is thought to play a critical role in modulating normal neuronal function and synaptic transmission making it particularly relevant in neuropharmacology.[7,8,9,10,11,12,13,14,15,16] Its biology is predicted to be distinct from the other group III mGlu members due to its specific localization and its remarkably low affinity for glutamate compared to $mGlu_4$ and $mGlu_8$,[17,18,19] being only activated by millimolar (i.e. non-physiological) glutamate concentrations.

Studies using $mGlu_7$ receptor knock-out animals have provided important insights into the potential role of this receptor in numerous neurological and psychiatric disorders including schizophrenia,[10] depression,[20] anxiety,[21] and epilepsy.[22] Likewise numerous polymorphisms in the metabotropic glutamate receptor 7 gene (GRM7) have been linked to autism, depression, ADHD, and schizophrenia.[23,24,25,26] Academic groups and pharmaceutical companies have mostly concentrated on the development of ligands acting at group I and II receptors. Both orthosteric and allosteric ligands have progressed into clinical trials with encouraging results in various indications.[27] However, much less has been discovered regarding the activation or blockade of group III mGlu receptors,[16] amongst which $mGlu_7$ is arguably the least explored. This is partly due to the difficulties to develop tool compounds with appropriate selectivity profiles to aid in performing proof-of-concept studies regarding the therapeutic potential of each receptor subtype.[28] After the discovery of early selective group III receptor orthosteric agonists, such as L-2-amino-4-phosphonobutyric acid (L-AP4),[29,30] research efforts shifted towards the search of allosteric modulators. Allosteric ligands could offer numerous advantages over orthosteric ligands such as improved subtype selectivity amongst other members of the mGlu receptor family, more drug-like structures, and the ability to enhance receptor activity only when and where biologically needed.[31,32] Thus, *N*,*N*-dibenzhydrylethane- 1,2-diamine dihydrochloride (AMN082,

1) was identified as the first $mGlu_7$ receptor-selective allosteric agonist, that is, a ligand that is capable of directly activating the receptor from an allosteric site in the absence of an orthosteric agonist,[33] and has been widely used to interrogate the role and therapeutic potential of the $mGlu_7$ receptor (Figure 1).[34,35] AMN082 has been shown to directly activate $mGlu_7$ via an allosteric binding site acting as the first full allosteric agonist at an mGlu receptor.[9] Unlike positive allosteric modulators (PAMs) that usually increase the potency of orthosteric agonists, AMN082 has little or no effects on the potency of glutamate or the orthosteric group III selective agonist L-AP4.[28]. However, AMN082 is rapidly metabolized in vivo. *N*-benzhydrylethane-1,2-diamine, a major metabolite of this compound, has been shown to exhibit significant off-target effects via modulation of multiple monoamine transporters. Concerns have been raised that interaction with these off-targets could confound the outcomes from in vivo behavioral models by producing a non-$mGlu_7$ receptor-mediated response.[36] This limits its value as a tool compound and there is a significant need for improving $mGlu_7$ allosteric ligands.

Recently, Niswender *et al.* have described the first group III selective PAMs: VU0422288 (**2**) and VU0155094 (**3**).[37] Unlike allosteric agonist, a PAM potentiates an agonist-mediated receptor response.[33] Despite the lack of selectivity for $mGlu_7$ vs $mGlu_4$ and $mGlu_8$ both compounds represented valid tools to selectively probe a role for $mGlu_7$ due to its restricted expression in SC-CA1 synapses in adult animals. More recently, Lindsley et al. identified a series of pyrazolo[1,5-a]pyrimidines from a high throughput screen (HTS) that display a range of group III mGlu receptors selectivity[38]. Among these, the selective $mGlu_{7/8}$ PAM VU6005649 (**4**) demonstrated pro-cognitive effects on associative learning in a mouse contextual fear conditioning model. Here we report a new chemical series of $mGlu_7$ allosteric modulators. The series was optimized with the help of modelling the binding mode in the 7-transmembrane (7TM) domain of the $mGlu_7$ receptor. With pIC_{50} values of around 7 and relatively good physicochemical properties they offer potential for future lead optimization.

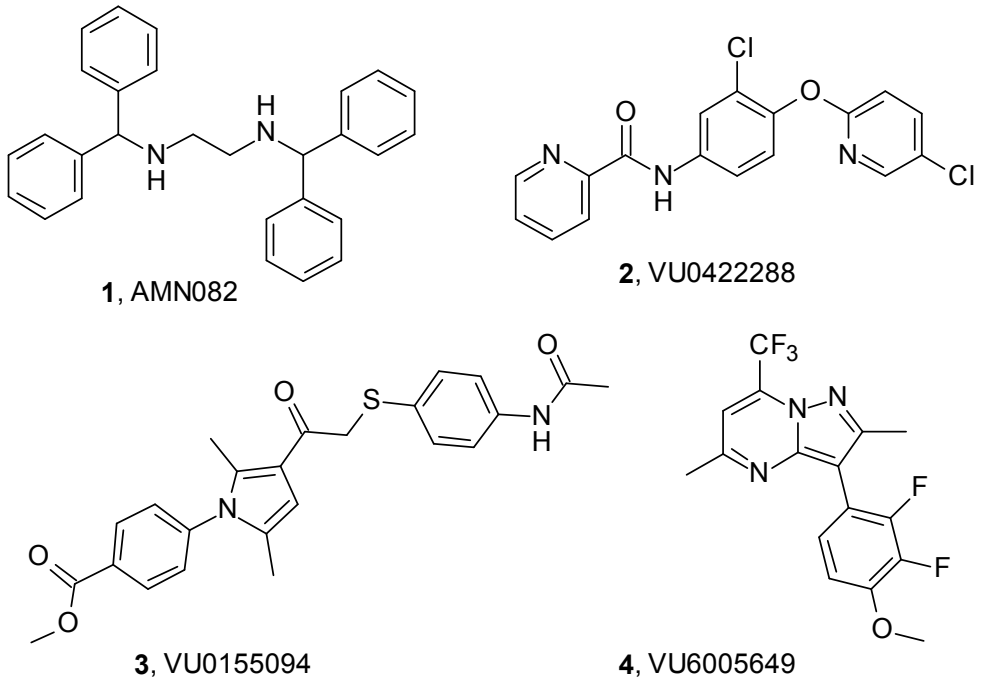

Figure 1. Structures of group III mGlu allosteric agonists and PAMs

RESULTS AND DISCUSSION

We have recently reported on our efforts to identify novel small molecule ligands for $mGlu_7$ receptors by means of a virtual screen using proteochemometric modelling.[39] The approach used a combined in-house and public dataset of around 2800 compounds tested for activation or inhibition of signaling versus mGlu receptors. The data was used to build computational models that could predict $mGlu_7$ receptor activity of molecules from the Janssen corporate compound collection. This method was well suited to take advantage of the many bioactive molecules for targets such as $mGlu_1$, $mGlu_2$ and $mGlu_5$ receptors, and use this information to make predictions for a similar but less explored receptor such as $mGlu_7$. Compounds were selected and screened and one particularly interesting hit molecule **A**, referred to as molecule 3 in the original report, was identified (Figure 2).[3938] The hit showed structural similarity to AMN082 due to the presence of a similar distal benzhydryl group. This molecule **A** was followed up with immediate close-analogue searching. In brief, the analogue searches used 2D ECFP6 circular topological fingerprints and Tanimoto similarity well suited for similarity comparison. The closest compounds from the Janssen compound library, as well as analogues from substructure searches were

combined giving over 400 unique compounds that were selected and screened. This led to compound **5** that was an acceptable micromolar starting point to begin building structure activity relationships (SAR).

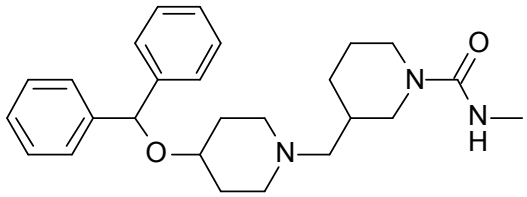

A
$mGlu_7$ pEC_{50} 5.8; E_{max} 76%

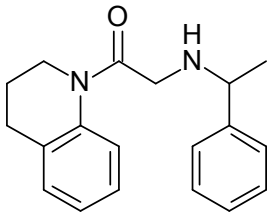

5
$mGlu_7$ pEC_{50} 5.8; E_{max} 58%

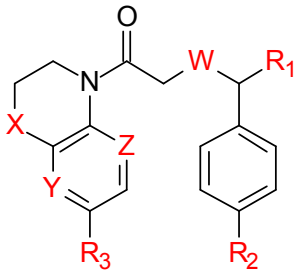

This work

Figure 2. Structure of hits **A** and **5** derived from an $mGlu_7$ receptor virtual screen, and the general scheme of $mGlu_7$ allosteric agonists presented here.

Chemistry

The majority of the analogues **5-16**, **19** and **23-25** were prepared in one step via alkylation of the corresponding commercially available haloacetamides (**26a-f**) with an array of benzylamines and benzyl alcohols (**27a-j**) as outlined in Scheme 1. Additionally, compound **17** was synthesized as shown in Scheme 2. Thus, *N*-alkylation of *tert*-butyl *N*-(2-amino-2-phenylethyl)carbamate (**27k**) with the chloroacetamide (**26e**) afforded compound **28**. Subsequent Boc protection of the benzylic nitrogen led to the corresponding bis-Boc derivative (**29**) that was treated with MeI to afford the intermediate compound **30.** Finally, removal of the Boc protecting groups in acidic media led to the target compound **17**.

Compounds **18**, **20-22** were following a reaction sequence similar to that described for the synthesis of **17** (Scheme 3). Alkylation of the benzylalcohols **27l**, **m** with chloroacetamides (**26e**, **f**) to obtain **31a**, **b**, followed by coupling with 2-nitrobenzenesulfonyl chloride yielded intermediates **32a**, **b**. Subsequent alkylation of the sulfonamide nitrogen yielded intermediates **34a-d**. Removal of the nosyl group from intermediates **34a-c** led to the final compounds **18**, **20** and **21** in low to moderate yields. Finally compound **22** was obtained from intermediate **34d** by Suzuki cross coupling with pyridyl-4-boronic acid and subsequent cleavage of the N-nosyl protecting group.

The chemical structures of compounds **5**–**25** are shown in Tables 1 and 2.

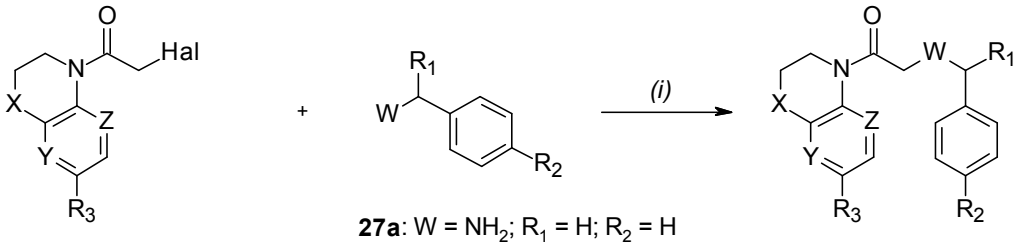

26a: Hal = Br; X,Y,Z = CH; R_3 = H
26b: Hal = Cl; X,Z = CH; Y = N; R_3 = H
26c: Hal = Cl; X,Y = CH; Z = N; R_3 = H
26d: Hal = Cl; X = O; Y,Z = CH; R_3 = H
26e: Hal = Cl; X,Y,Z = CH; R_3 = H
26f: Hal = Cl; X,Y,Z = CH; R_3 = F

27a: W = NH_2; R_1 = H; R_2 = H
27b: W = NH_2; R_1 = Ph; R_2 = H
27c: W = NH_2; R_1 = CyPr; R_2 = H
27d: W = NH_2; R_1 = CH_3; R_2 = H
27e: W = NH_2; R_1 = CF_3; R_2 = H
27f: W = NH_2; R_1 = CH_2OH; R_2 = H
27g: W = NH_2; R_1 = CH_2OCH_3; R_2 = H
27h: W = OH; R_1 = $CH_2N(CH_3)_2$; R_2 = H
27i: W = OH; R_1 = CH_2NHCH_3; R_2 = F
27j: W = OH; R_1 = CH_2NHCH_3; R_2 = H

5-16; 19; 23-25

Scheme 1. *Reagents and conditions:* (i) a) Et_3N, CH_3CN, rt, 3 h, 10-49% for **6-9** and **12-16** or b) NaH, DIPEA, DMPU, rt, 3 days, 4-17% for **5**[40], **10** and **11** or c) NaH, THF, rt, 16 h, 25-38% for **19** and **23-25**.

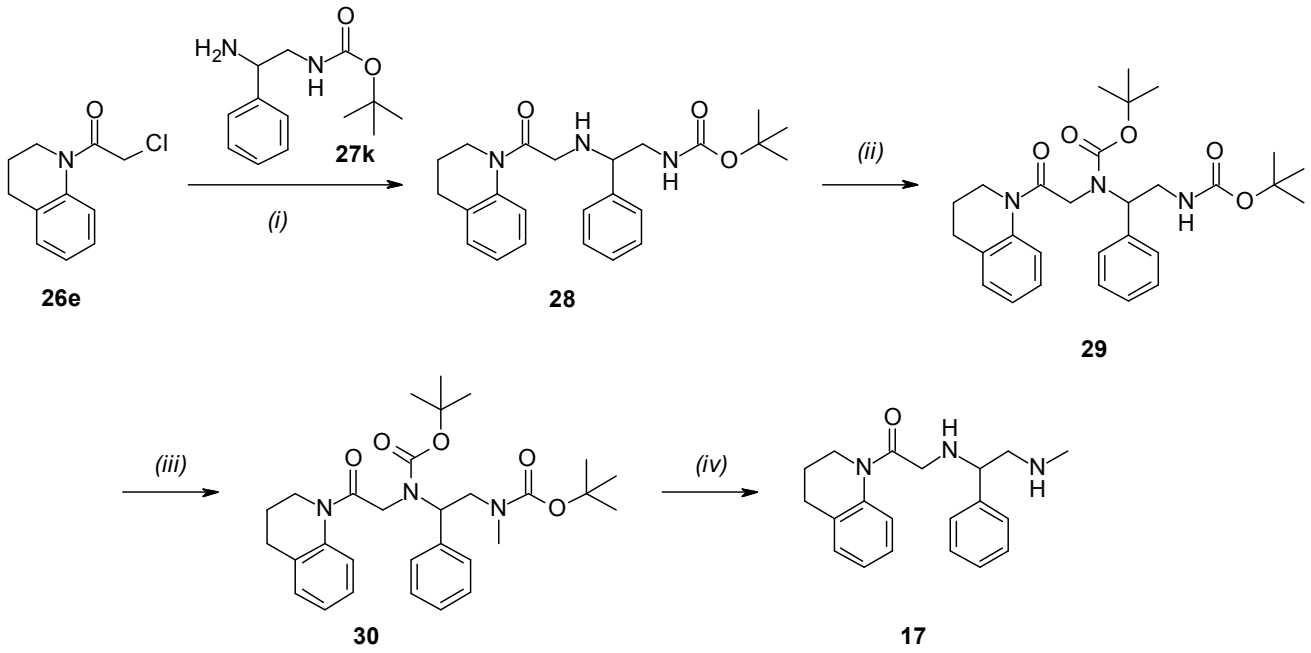

Scheme 2. *Reagents and conditions:* (i) K_2CO_3, CH_3CN, 80 ºC, 16 h, 51%; (ii) BOC_2O, Et_3N, DCM, rt, 24 h, 47 %; (iii) MeI, NaH, THF, rt. 48 h, 51% (iv) HCl, rt, 85%.

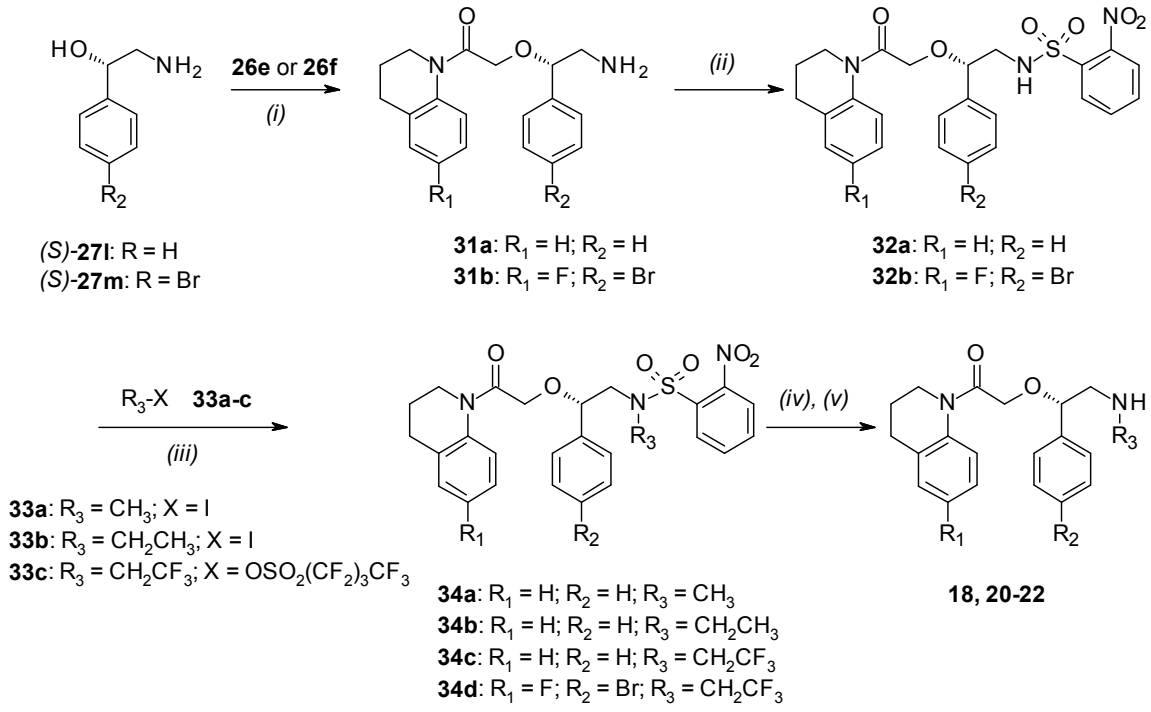

Scheme 3. *Reagents and conditions:* (i) NaH, THF, 0 ºC to rt, 24 h, 61-100 %; (ii) *o*-nitrobenzenosulfonyl chloride, Et_3N, DCM, rt, 16 h, 84 %; (iii) Cs_2CO_3, THF, 0 ºC to rt, 70-99 %; (iv) **34a-c**, 2-mercaptoethanol, LiOH, DMF, rt, 16 h, 14-77 %, for **18**, **20** and **21**; (v) a) **34d**, 4-pyridinyl

boronic acid, $PdCl_2(dppf)_2$, Na_2CO_3, 1,4-dioxane, 90 ºC, 6 h, 87 %; b) 2-mercaptoethanol, LiOH, DMF, rt, 16 h, 57 % for **22**.

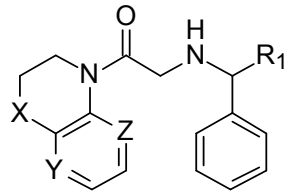

Table 1. Functional activity and metabolic stability of representative $mGlu_7$ receptor allosteric agonists **1, 5-17**[a].

Entry	X	Y	Z	R_1	$mGlu_7$ pEC_{50}[a]	$mGlu_7$ E_{max}(%)[a]	cLogP[b]	CL_{int} microsomes (μL/min)/mg)(h/r)[c]
1	-	-	-	-	6.8	62	5.9	nt
5	CH_2	CH	CH	(*RS*)-CH_3	5.8	58	3.7	nt
6	CH_2	CH	CH	*(R)*-CH_3	5.59	69	3.7	>346/>346
7	CH_2	CH	CH	*(S)*-CH_3	6.06	90	3.7	>346/>346
8	CH_2	CH	CH	H	<4.5	44	3.3	68/>346
9	CH_2	CH	CH	Ph	6.66	97	4.7	>346/>346
10	CH_2	CH	CH	(*RS*)-CyPr	6.62	73	4.1	>346/>346
11	CH_2	CH	CH	*(RS)*-CF_3	6.19	98	4.1	>346/>346
12	CH_2	CH	CH	*(S)*-CH_2OH	5.63	65	2.5	147/>346
13	CH_2	N	CH	*(S)*-CH_2OH	<4.3	40	1.0	nt
14	CH_2	CH	N	*(S)*-CH_2OH	<4.3	3	1.0	nt
15	O	CH	CH	*(S)*-CH_2OH	5.62	46	1.9	43/240
16	CH_2	CH	CH	*(S)*-CH_2OCH_3	5.75	58	3.3	>346/>346
17	CH_2	CH	CH	*(S)*-CH_2NHCH_3	6.14	77	2.9	90/>346

[a]Most values represent the mean for at least two experiments, [b]cLogP calculated with Biobyte software, [c](h/r) human/rat.

SAR and model discussion

Structural analogy of the original virtual screening hit **A** as well as molecule **5** with AMN082 prompted us to start our SAR studies by exploring the alpha position of the benzylamine (see Figure 2).

Compounds **5**–**25** were evaluated for $mGlu_7$ agonistic activity (see methods) and data is shown in Table 1 and 2. As a point of reference, compound **1** (AMN082) had a pEC_{50} of 6.8 with 62% potentiation in our agonist assay compared with a reported EC_{50} of 64 nM.[8] Replacement of the alkyl linker of compound **5** with a single enantiomer chain produced enantiomers **6** (*R*) and **7** (*S*) with pEC_{50} values of 5.59 and 6.06 respectively. Although relatively close in activity, the preference for the *S*-isomer conformation in the linker region led us to maintain this for further derivative synthesis.

Potency was remarkably improved by installation of a phenyl group in **9** that showed a 0.86 log unit increase in potency (pEC_{50} = 6.66) compared to initial hit **5**, Table 1. Compound **9** had comparable activity to AMN082 and also confirmed the similarity with the benzhydryl amino fragment present in AMN082. The activity of **9** and similarity with AMN082 provided confidence to consider additional computational methods to help design new compounds. Recently, we have shown how combined experimental and computational approaches can be used to generate binding mode hypotheses for different series of $mGlu_2$ receptor PAMs and NAMs.[41,42,43,] A robust binding mode was proposed and further study led to a hypothesis of the origin of functional activity for mGlu allosteric modulators. They achieve their effect by modifying the movement of amino acids in crucial positions of the GPCR 7TM, referred to as the Triger and Transmission switches.[44] Amino acids at the same positions in TMs 3, 5, and 6 are known to be important for class A activation.[45,46]

Based on this knowledge of mGlu receptor modelling and allosteric ligand function we derived a structure-based hypothesis for the binding mode of $mGlu_7$ receptor allosteric agonist **9**. Firstly, a structural model of the active state of the $mGlu_7$ receptor (Uniprot code Q14831) 7TM was built. The crystal structure of the $mGlu_5$ receptor[47] (PDB 4OO9, 50% sequence identity in the 7TM region) was used as a template for most of the receptor. Extracellular loop 2, which is not resolved in the $mGlu_5$ structure, was modelled using the $mGlu_1$ receptor structure[48] (PDB 4OR2). To model the active state,

the conformation of the intracellular TM6 of mGu_7 receptor (N785-M794) was modified based on the active conformation in the β_2AR-Gs complex[49] (PDB 3SN6). Models were constructed with MOE (Chemical Computing Group, https://www.chemcomp.com/). The final model was chosen as the best quality result having a low RMSD (root mean square deviation) to the average models (i.e. not a structural outlier), no outliers from a Ramachandran dihedral or bond length plots, correct stereochemistry and no high energy contacts. These factors along with the sequence identity to the $mGlu_5$ template in the 7TM region provided confidence in the final model. Molecule **9** was docked using the MOE induced fit docking approach. The binding site and flexible amino acids were defined as all the atoms of the $mGlu_7$ sidechains within a 6 Å radius around the position of the allosteric binding site. The allosteric site was defined based on structural alignment to the $mGlu_1$ crystal structure bound with FITM[47] (PDB 4OR2). A tether factor (10x) was used to constraint sidechain flexibility and results were submitted to further minimization.

Docking of **9** delivered multiple binding modes as expected, but one was common to the best scoring solutions, Figure 3. In this orientation, the benzhydrylamine group penetrated deepest into the receptor. The 7TM binding cavity was hydrophobic and interestingly contains as many as three methionine residues making direct contact with the ligand, $M666^{3.40c}$, $M767^{5.51c}$, and $M829^{7.36c}$. The upper part of the binding pocket was lined with lipophilic amino acids interacting with the tetrahydroquinoline, $L662^{3.36c}$, $I756^{5.40c}$, $L760^{5.44c}$, $W801^{6.50c}$, $F804^{6.53c}$ and $L825^{7.32c}$. The amide carbonyl of **9** was predicted to act as a hydrogen bond acceptor from the side chain of $S763^{5.47c}$. Meanwhile the benzhydryl group entered the lower lipophilic pocket, surrounded by the three methionine residues and sitting on top of the mGlu receptor conserved and functionally important $Y670^{3.44c}$. The amino acids $M666^{3.40c}$, $S763^{5.47c}$, $W801^{6.50c}$ are at the same structural position as the side-chains associated with the trigger switch of $mGlu_2$ PAM activity,[42] hence it was consistent to see similar interactions with the $mGlu_7$ allosteric agonists here. With only a limited amount of SAR it was difficult at this stage to confirm the binding mode, thus we designed molecules to test it further.

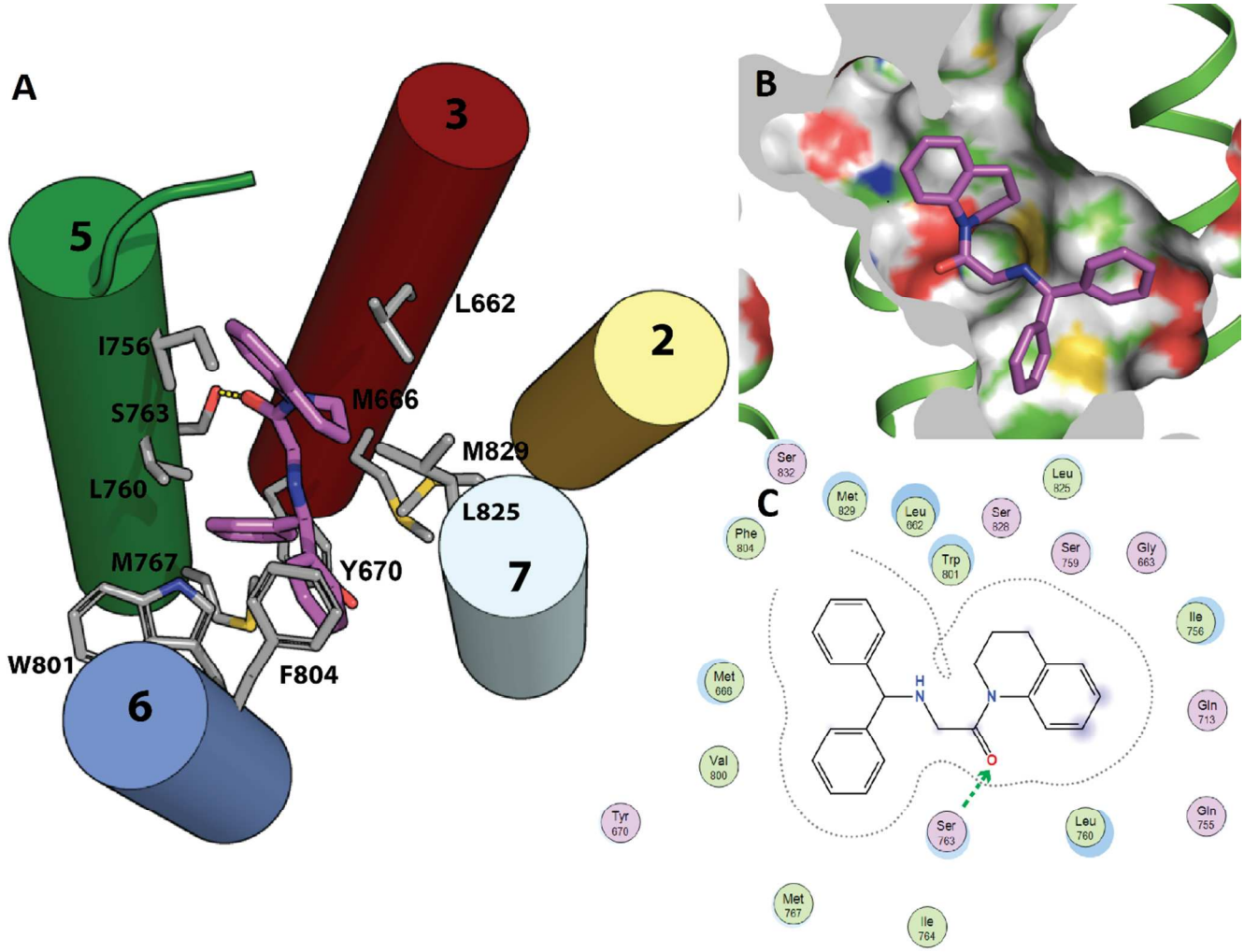

Figure 3. The docked binding mode of compound **9** at the 7TM domain of the $mGlu_7$ receptor. A: The binding mode with the benzhydryl group penetrating deepest, TM helices are numbered, and amino acids labelled. B: Cut-through surface side view of the ligand binding cavity, coloring is according to nearby atom types. C: The 2D interaction map showing more details of the amino acids surrounding the ligand.

With this binding mode in mind we designed smaller and less lipophilic groups to replace the benzhydryl substituent. Thus, compounds **10-12** were synthesized to investigate if more drug-like motifs were tolerated. Removing the R_1 methyl group, as shown in **8**, resulted in a loss of potency. The replacement of the phenyl group by cyclopropyl produced **10**, that exhibited potency similar potency to **9** (**10**: pEC_{50} = 6.62 vs **9**: pEC_{50} = 6.66). Slight reduction in potency was found with the CF_3 substitution

(**11**: pEC_{50} = 6.19). The surface view in Figure 3B suggested that more polar groups may be permitted in the deeper part of the pocket and interact with acceptor groups represented by the red-surface coloring. Interestingly, introduction of a group such as CH_2OH (**12**) did indeed result in active compounds (pEC_{50} = 5.63). The activity seen for compound **12** stimulated us to exploit the CH_2OH substitution in combination with other variations. Thus, starting from **12**, we reduced the lipophilicity of the bicyclic tetrahydroquinoline warhead. Unfortunately, analogues **13** and **14** in which a N-atom is introduced into the benzopyran nucleus had a deleterious effect on activity. These results were likely due to unfavorable interactions with the many lipophilic amino acids around this upper pocket. However, the 1,4-benzoxazine **15** that had the oxygen atom at the benzylic position of the bicyclic core showed comparable activity to that of its corresponding carbon analogue (**12**: pEC_{50} = 5.63 vs **15**: pEC_{50} = 5.62). The overall favored tetrahydroquinoline group was kept intact for subsequent exploration. Further exploration of the deep pocket by introducing alternative heteroatom containing substituents, led to compounds **16** and **17**. The ether derivative displayed comparable potency to the alcohol **12** (**12**: pEC_{50} = 5.63 vs **16**: pEC_{50} = 5.75). Introduction of an aliphatic amine (**17**) was somewhat more favorable than methoxy (**(**pEC_{50} = 6.14) and also attractive from the druglike perspective for potentially improving solubility and reducing lipophilicity.

Table 2. Functional activity and metabolic stability of representative $mGlu_7$ receptor agonists **18-25**[a]

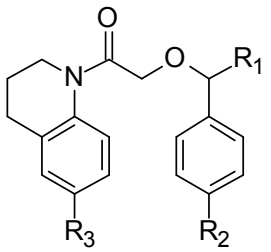

Entry	R_1	R_2	R_3	$mGlu_7$ pEC_{50}[a]	$mGlu_7$ E_{max}(%)[a]	cLogP[b]	CL_{int} microsomes (μL/min)/mg) (h/r)[c]
18	*(S)*-CH_2NHCH_3	H	H	6.96	71	3.0	80/>346
19	*(S)*-$CH_2N(CH_3)_2$	H	H	6.7	60	3.6	nt
20	*(S)*-$CH_2NHCH_2CH_3$	H	H	6.85	68	3.6	96/>346
21	*(S)*-$CH_2NHCH_2CF_3$	H	H	6.15	81	3.8	>346/>346
22	*(S)*-$CH_2NHCH_2CF_3$	4-pyridine	F	<4.3	5	4.6	nt
23	*(S)*-CH_2NHCH_3	F	H	5.83	47	3.2	54/>346
24	*(S)*- CH_2NHCH_3	H	F	6.33	57	3.2	68/>346
25	*(S)*-CH_2NHCH_3	F	F	5.76	32	3.3	42/>346

[a]Most values represent the mean for at least two experiments, [b]cLogP calculated with Biobyte software, [c](h/r) human/rat

The binding mode suggested the nitrogen in the central spacer was not essential, for instance it did not form any hydrogen bond or salt bridge interactions. We investigated this by modifying it to an ether spacer in compounds **18** to **25**, Table 2. Compound **18** conferred a remarkable increase in potency (pEC_{50} = 6.96) compared to its corresponding nitrogen version (**17**; pEC_{50} = 6.14). This promising increase motivated us to further expand SAR on the terminal amino group as exemplified with compounds **19-21**. Different N-alkyl groups were introduced unfortunately none of them displayed greater potency and activity was only slightly lower indicating flat SAR, neither driven by an increase in lipophilicity nor size. Interestingly, compound **22** having the appended pyridine was totally inactive compared to the similarly substituted compound **21**. This suggested that the receptor does not accommodate substituents larger than a methyl group in this region. This is consistent with the binding mode shown in Figure 3A, where the R_1 and R_2 groups penetrate deepest into the 7TM and larger groups would clash with the surface of the binding cavity, Figure 3B.

In the final set of experiments, a limited exploration was conducted to investigate the effects of electronic density on the phenyl rings of the tetrahydroquinoline or distal phenyl. Compounds **23-25** bearing fluorine atoms at the phenyl ring turned out to be less active compared to the non-substituted analogue **18**. Whilst **24** was the most active of the three (pEC_{50} = 6.33), analogue **25** containing two fluorine atoms was the least active (pEC_{50} = 5.76). This might suggest a role for the two aryls in stabilizing the binding mode by forming aromatic stacking interactions, or aliphatic C-H aromatic interactions for instance with $L662^{3.36c}$, $I756^{5.40c}$, $L825^{7.32c}$ which are favored by electron rich rings. Several compounds such as **9** and **11** showed higher E_{max} than the initial compounds such as AMN082 and **5**. Furthermore, compounds **7**, **9** and **11** with *(S)*-CH_3, phenyl or CF_3 showed relatively high E_{max} (90, 97 and 98 % respectively) and interestingly the *(R)*-CH_3 a lower E_{max} (69 %). Therefore, the R_1 pocket is important for functional effect. The R_1 substituents are interacting with amino acids $M666^{3.40c}$, $S763^{5.47c}$ and $W801^{6.50c}$. These amino acids are the $mGlu_7$ receptor equivalent of the 3 amino acids described as the Trigger switch in $mGlu_2$.[43] They sit one turn directly above the transmission switch and adopt different conformational behavior depending on the functional activity of the allosteric modulator. It seems likely that the $mGlu_7$ ligands here cause similar effects.

Receptor potency was improved quickly but metabolic stability studies in both human and rat liver microsomes (HLM, RLM) proved more challenging (Tables 1 and 2). Most of the compounds suffered from extensive metabolism in both species, particularly in rats. Slight improvement was observed with the introduction of polar groups as illustrated with compound **12** and even more so for **15**, suggesting a metabolic hot spot located at the benzylic position of the bicyclic core. As anticipated, compounds **16-21** having new potential metabolic sites did not exhibit any improvement. Reduction of electron density on the rings, via addition of electron-withdrawing groups, was not an effective strategy: compounds **23-25**, bearing fluorine atoms, showed only a subtle improvement in stability in humans.

Furthermore, as AMN082, compounds **5-25** do not affect Ca^{2+} responses in HEK293 cells co-expressing the human mGlu7 receptor and the promiscuous G protein Gα15 (data not shown). A same

complex pharmacological profile of AMN082 has been described before[50]. While all molecules were inactive against other mGlu receptors in this same read-out, we have not evaluated other receptor responses or cell populations, assuming selectivity towards other mGlu receptor subtypes ($mGlu_{1,2,3,4,5,6,8}$) remains as good as for AMN082, given their high similarity and shared binding mode.

Conclusion

A novel series of tetrahydroquinolines with $mGlu_7$ receptor allosteric agonistic activity has been described. Arising from a virtual screening hit, the molecules were rapidly optimized with the help of modelling the binding mode into a homology model of the Glu_7 receptor. Starting from hit **5**, a set of derivatives were synthesized allowing for a conclusive SAR study. Potency reached significant levels with pEC_{50} close to 7 for several examples. This compared favorably to the well-studied reference compound AMN082. Physicochemical properties were also improved, with examples such as **18** having lower lipophilicity than compared to AMN082, with LogP of 3 for **18** vs LogP of 5.9 for AMN082. Taken together, these results suggest promise for this tetrahydroquinolines series. However, the challenge remains to combine potency with metabolic stability. These studies are underway and will be the subject of future reports from our laboratories. Since it is only now that more selective $mGlu_7$ receptor agonists and antagonists have been identified, we expect this study can contribute to a clearer picture on the role of the $mGlu_7$ receptor over the coming years.

METHODS

Measurements of $mGlu_7$ agonist activity. Modulation of forskolin-induced cAMP accumulation was measured in human $mGlu_7$ receptor-expressing CHO cells using the Lance ® Ultra cAMP kit (Perkin Elmer). Cells were seeded at 2,000 cells/well in 384-well white Optiplates (Perkin Elmer). After addition of forskolin (2 μM), cells were incubated at room temperature for 30 min, followed by addition of Lance ® Ultra cAMP reagents and additional 60 min incubation at room temperature. Lance signal was measured on an Envision multilabel reader (Perkin Elmer). Agonist effects were picked up by a reduction in forskolin-induced cAMP production or consequently, an increase in Lance signal.

Liver Microsomal Stability. Microsomal stability studies were conducted on a Biomek FX robotic liquid handling workstation (Beckman Coulter, Brea, CA), which consists of a 96-channel pipet head, a 12-postion workstation deck, and a plate incubator. The test compound is incubated at a defined substrate concentration (typically 1 μM) in liver microsomes from human and rat across a time course (typically 0, 5, 10, 20, 40, and 60 minutes). The reaction was brought to 37 °C and initiated by adding NADPH to a final concentration of 1 mM. The reaction is terminated by addition of a suitable organic solvent (typically, acetonitrile, methanol or DMSO). The samples are centrifuged prior to analysis by LC-MS/MS analysis. The relative amount of parent compound remaining in the active incubations vs. the control incubations (t=0 mins) for each compound is measured by peak area comparison. The predicted hepatic clearance was derived from the intrinsic clearance value using equations from the well-stirred model (Curr. Drug Metab. 2008, 9, 940−951), where protein binding in plasma and microsomal proteins is assumed to be similar and the blood to plasma concentration ratio is assumed to be 1.

Chemistry. Unless otherwise noted, all reagents and solvents were obtained from commercial suppliers and used without further purification. Thin layer chromatography (TLC) was carried out on silica gel 60 F254 plates (Merck). Flash column chromatography was performed on silica gel, particle size 60 Å, mesh = 230−400 (Merck), under standard techniques. Microwave assisted reactions were performed in a single-mode reactor, Biotage Initiator Sixty microwave reactor (Biotage), or in a multimode reactor, MicroSYNTH Labstation (Milestone, Inc.). Nuclear magnetic resonance (NMR) spectra were recorded with either a Bruker DPX-400 or a Bruker AV-500 spectrometer (broaduker AG) with standard pulse sequences NMR data operating at 400 and 500 MHz, respectively, using $CDCl_3$ and DMSO-d6 as solvents. Chemical shifts (δ) are reported in parts per million (ppm) downfield from tetramethylsilane (δ = 0). Coupling constants are reported in hertz. Splitting patterns are defined by s (singlet), d (doublet), dd (double doublet), t (triplet), q (quartet), quin (quintet), sex (sextet), sep (septet), or m (multiplet). Liquid chromatography combined with mass spectrometry (LC−MS) was performed either on a HP 1100 HPLC system (Agilent Technologies) or Advanced Chromatography Technologies

system composed of a quaternary or binary pump with degasser, an autosampler, a column oven, a diode array detector (DAD), and a column as specified in the respective methods. Flow from the column was split to a MS spectrometer. The MS detector was configured with either an electrospray ionization source or an ES-CI dual ionization source (electrospray combined with atmospheric pressure chemical ionization). Nitrogen was used as the nebulizer gas. Data acquisition was performed with MassLynx-Openlynx software or with Chemsation-Agilent Data Browser software. Retention time (tR) is expressed in min. Gas chromatography combined with mass spectrometry (GC−MS) was performed using a 6890 series gas chromatograph (Agilent Technologies) system comprising a 7683 series injector and autosampler, a column oven, and a J&W HP-5MS coupled to a 5973N MSD mass selective detector (single quadrupole, Agilent Technologies). The MS detector was configured with an electronic impact ionization source/chemical ionization source (EI/CI). EI low-resolution mass spectra were acquired by scanning from 50 to 550 at a rate of 14.29 scans/s. The source temperature was maintained at 230 °C. Helium was used as the nebulizer gas. Data acquisition was performed with Chemstation-Open Action software. Melting point (mp) values are peak values and were obtained with experimental uncertainties that are commonly associated with this analytical method and were determined in open capillary tubes on a Mettler FP62 apparatus with a temperature gradient of 10 °C/min. Maximum temperature was 300 °C.

Purities of all new compounds were determined by analytical reverse phase (RP) HPLC using the area percentage method on the UV trace recorded at a wavelength of 254 nm and were found to have ≥95% purity unless otherwise specified.

Supercritical fluid chromatography (SFC) was performed using Analytical system from Berger instrument comprising a FCM-1200 dual pump fluid control module for delivering CO_2 and modifier, a CTC Analytics automatic liquid sampler, a TMC-20000 thermal control module for column heating from room temperature to 80ºC. An Agilent 1100 UV photodiode array detector equipped with a high-pressure flow cell standing up to 400 bars was used. Flow from the column was split to a MS spectrometer. The MS detector was configured with an atmospheric pressure ionization source. The

following ionization parameters for the Waters ZQ mass spectrophotometer are: corona: 9μa, source tem: 140ºC, cone: 30V, probe temp 450ºC, extractor 3 V, desolvatation gas 400Lhr, cone gas 70 L/hr. Nitrogen was used as the nebulizer gas. Data acquisition was performed with a Waters-Micromass MassLynx-Openlynx data system.

2-(benzylamino)-1-(1,2,3,4-tetrahydroquinolin-1-yl)ethan-1-one (8). A mixture of **26a** (0.160 g, 0.63 mmol), **27a** (0.135 g, 1.26 mmol), and Et_3N (0.175 mL, 35.2 mmol) in CH_3CN (1.8 mL) was stirred at room temperature for 3h and then concentrated in vacuo. The crude product was purified by RP HPLC (Stationary phase: C18 XBridge 30 x 100 mm 5 um), Mobile phase: Gradient from 67% 0.1% NH_4CO_3H/NH_4OH pH 9 solution in Water, 33% CH_3CN to 50% 0.1% NH_4CO_3H/NH_4OH pH 9 solution in Water, 50% CH_3CN) to give **8** as a colorless oil (0.087 g, 49%). ^{1}H NMR (500 MHz, $CDCl_3$) δ 7.18-7.35 (m, 6H), 7.04-7.17 (m, 3H), 3.76 (br s, 4H), 3.56 (s, 2H), 2.70 (br t, *J*=6.50 Hz, 2H), 2.36 (s, 1H), 1.94 (quin, *J*=6.57 Hz, 2H). LCMS: m/z 281 $[M + H]^+$, *t*R = 1.90 min.

2-(diphenylmethylamino)-1-(1,2,3,4-tetrahydroquinolin-1-yl)ethan-1-one (9). Starting from **26a** (0.183 g, 0.72 mmol) and **27b** (0.158 g, 0.87 mmol) and following the procedure described for **8**, compound **9** was obtained as a yellow solid (0.063 g, 25%). ^{1}H NMR (500 MHz, $CDCl_3$) δ 7.39 (br d, *J*=7.22 Hz, 4H), 7.23-7.32 (m, 6H), 7.15-7.23 (m, 2H), 6.98-7.14 (m, 3H), 4.85 (br s, 1H), 3.58-3.88 (m, 2H), 3.52 (s, 2H), 2.69 (br s, 2H), 1.93 (quin, *J*=6.57 Hz, 2H). LCMS: m/z 357 $[M + H]^+$, *t*R = 2.94 min.

***(RS)*-2-(1-methy-1-cyclopropyl)-benzylamino)-1-(1,2,3,4-tetrahydroquinolin-1-yl)ethan-1-one (1)**. Starting from **26a** (0.683 g, 2.69 mmol) and **27c** (0.247 g, 1.34 mmol) and following the procedure described for **8**, compound **10** was obtained as a yellow solid (0.075 g, 17%). ^{1}H NMR (500 MHz, $CDCl_3$) δ 7.19-7.36 (m, 6H), 7.01-7.13 (m, 3H), 3.69 (br s, 2H), 3.43 (q, *J*=15.80 Hz, 2H), 2.80 (br d, *J*=8.67 Hz, 1H), 2.68 (br t, *J*=6.36 Hz, 2H), 1.84-2.00 (m, 2H), 1.61 (br s, 3H), 0.97-1.16 (m, 1H), 0.53-0.69 (m, 1H), 0.29-0.46 (m, 1H), 0.13-0.26 (m, 1H). LCMS: m/z 321 $[M + H]^+$, *t*R = 2.42 min.

***(RS)*-2-(1-methylbenzylamino)-1-(1,2,3,4-tetrahydroquinolin-1-yl)ethan-1-one (5).** Diisopropylethylamine (0.246 mL, 1.42 mmol) was added to a solution of *(RS)*-**27d** hydrochloride (0.15 g, 0.95 mmol) in 1,3-dimethyl-3,4,5,6-tetrahydro-2(1H)-pyrimidinone (DMPU) (3 mL) at 0ºC. The

mixture was stirred for 5 min and NaH (0.086 mg, 2.14 mmol) was added portion wise. Then, a solution of **26a** (0.62 g, 1.9 mmol) in DMPU (2 mL) was added dropwise and the resulting mixture was gradually warmed to room temperature and stirred for 3 days. The mixture was diluted with water and extracted with EtOAc. The organic layer was washed with brine, dried over anhydrous Na_2SO_4, and concentrated in vacuo. The crude was purified by flash column chromatography (silica gel, EtOAc in DCM, 0/100 to 10/90) to give **5** as a pale brown oil (0.124 g, 17%). ^{1}H NMR (500 MHz, $CDCl_3$) δ 7.21 (m, 6H), 7.01-7.14 (m, 3H), 3.52-4.00 (m, 3H), 3.33-3.46 (m, 2H), 2.68 (br t, *J*=6.50 Hz, 2H), 1.83-1.99 (m, 3H), 1.37 (d, *J*=6.65 Hz, 3H). LCMS: m/z 295 $[M + H]^+$, *t*R = 2.13 min.

(R)-**2-(1-methylbenzylamino)-1-(1,2,3,4-tetrahydroquinolin-1-yl)ethan-1-one (6).** Starting from **26a** (0.436 g, 1.72 mmol) and (*R*)-**27d** (0.437 mL, 3.43 mmol) and following the procedure described for **8**, compound **6** was obtained as a colorless oil (0.215 g, 43%). ^{1}H NMR (400 MHz, $CDCl_3$) δ 7.16-7.34 (m, 6H), 7.01-7.14 (m, 3H), 3.50-3.94 (m, 3H), 3.34-3.46 (m, 2H), 2.68 (br t, *J*=6.59 Hz, 2H), 2.04-2.55 (br s, 1H), 1.81-2.03 (m, 2H), 1.37 (d, *J*=6.70 Hz, 3H). LCMS: m/z 295 $[M + H]^+$, *t*R = 2.19 min.

(S)-**2-(1-methylbenzylamino)-1-(1,2,3,4-tetrahydroquinolin-1-yl)ethan-1-one (7).** Starting from **26a** (0.450 g, 1.77 mmol) and (*S*)-**27c** (0.492 mL, 3.54 mmol) and following the procedure described for **8**, compound **7** was obtained as a colorless oil (0.124 g, 24%). ^{1}H NMR (500 MHz, $CDCl_3$) δ 6.43-8.06 (m, 9H), 4.17 (br s, 1H), 3.38-3.99 (m, 5H), 2.66 (br s, 2H), 1.79-2.11 (m, 2H), 1.71 (br d, *J*=6.65 Hz, 3H). LCMS: m/z 295 $[M + H]^+$, *t*R = 2.19 min.

(RS)-**2-(1-trifluoromethylbenzylamino)-1-(1,2,3,4-tetrahydroquinolin-1-yl)ethan-1-one (11).** Starting from **26a** (0.272 g, 1.07 mmol) and (*RS*)-**27e** (0.113 g, 0.535 mmol) and following the procedure described for **5**, compound **11** was obtained as a colorless oil (0.008 g, 4%). ^{1}H NMR (500 MHz, $CDCl_3$) δ 7.30-7.46 (m, 4H), 6.78-7.30 (m, 5H), 4.22 (br d, *J*=5.49 Hz, 1H), 3.31-4.02 (m, 4H), 2.51-2.94 (m, 3H), 1.80-2.01 (m, 2H). LCMS: m/z 349 $[M + H]^+$, *t*R = 2.60 min.

(S)-**2-(1-hydroxymethylbenzylamino)-1-(1,2,3,4-tetrahydroquinolin-1-yl)ethan-1-one (12)**. Starting from **26a** (0.256 g, 1 mmol) and (*S*)-**27f** (0.166 mL, 1.21 mmol) and following the procedure

described for **8**, compound **12** was obtained as a white solid (0.067 g, 21%). ^{1}H NMR (400 MHz, $CDCl_3$) δ 6.51-7.65 (m, 9H), 3.24-4.11 (m, 7H), 2.22-3.21 (m, 4H), 1.80-2.08 (m, 2H). LCMS: m/z 311 $[M + H]^+$, *t*R = 1.71 min.

(S)-**2-(1-hydroxymethylbenzylamino)-1-(1,2,3,4-tetrahydro-1,5-naphthyridin-1-yl)ethan-1-one (13)**. Starting from **26b** (0.200 g, 0.95 mmol) and (*S*)-**27f** (0.130 g, 0.95 mmol) and following the procedure described for **8**, compound **13** was obtained as a yellow oil (0.080 g, 26%). ^{1}H NMR (400 MHz, $CDCl_3$) δ ppm 1.86 - 2.12 (m, 2 H), 2.94 (t, *J*=6.78 Hz, 2 H), 3.39 - 3.95 (m, 7 H), 7.08 (dd, *J*=8.03, 4.77 Hz, 1 H), 7.25 - 7.38 (m, 5 H), 8.28 (dd, *J*=4.77, 1.51 Hz, 1 H). LCMS: m/z 312 $[M + H]^+$, *t*R = 2.35 min.

(S)-**2-(1-hydroxymethylbenzylamino)-1-(1,2,3,4-tetrahydro-1,8-naphthyridin-1-yl)ethan-1-one (14)**. Starting from **26c** (0.150 g, 0.712 mmol) and (*S*)-**27f** (0.085 g, 0.62 mmol) and following the procedure described for **8**, compound **14** (0.012 g, 12%). ^{1}H NMR (400 MHz, D_2O) δ 9.05 (d, *J*=6.62 Hz, 1H), 7.50 (d, *J*=7.50 Hz, 1H), 7.17-7.40 (m, 5H), 7.10 (t, *J*=7.28 Hz, 1H), 4.31-4.42 (m, 1H), 4.17 (s, 2H), 3.88-4.06 (m, 2H), 3.73 (t, *J*=5.51 Hz, 2H), 2.83 (br. s., 2H), 1.98 (d, *J*=5.29 Hz, 2H). LCMS: m/z 312 $[M + H]^+$, *t*R = 3.085 min.

(S)-**2-(1-hydroxymethylbenzylamino)-1-(3,4-dihydro-2H-benzo[*b*][1,4]oxazin-1-yl)ethan-1-one (15)**. Starting from **26d** (0.130 g, 0.614 mmol) and (*S*)-**27f** (0.084 g, 0.61 mmol) and following the procedure described for **8**, compound **15** (0.021 g, 11%). ^{1}H NMR (400 MHz, $CDCl_3$) δ ppm 3.45 - 3.60 (m, 3 H), 3.62 - 3.82 (m, 3 H), 4.17 (t, *J*=4.77 Hz, 3 H), 6.67 - 6.87 (m, 2 H), 6.94 - 7.05 (m, 1 H), 7.18 - 7.36 (m, 6 H). LCMS: m/z 313 $[M + H]^+$, *t*R = 4.133 min.

(S)-**2-(1-methoxymethylbenzylamino)-1-(1,2,3,4-tetrahydroquinolin-1-yl)ethan-1-one (16)**. Starting from **26a** (0.085 g, 0.334 mmol) and (*S*)-**27g** (0.061 mg, 0.401 mmol) and following the procedure described for **8**, compound **16** was obtained as a white solid (0.045 g, 41%). ^{1}H NMR (400 MHz, $CDCl_3$) δ ppm 1.92 (tq, *J*=12.91, 6.62 Hz, 3 H) 2.67 (t, *J*=6.40 Hz, 3 H), 3.35 - 3.41 (m, 5 H),

3.43 - 3.54 (m, 3 H), 3.57 - 3.84 (m, 2 H), 3.86 - 3.97 (m, 1 H), 6.97 - 7.13 (m, 1 H), 7.19 - 7.38 (m, 1 H). LCMS: m/z 325 $[M + H]^+$, *t*R = 3.69 min.

(S)-**2-(1-(N-BOC-aminomethylbenzylamino)-1-(1,2,3,4-tetrahydroquinolin-1-yl)ethan-1-one (28).** A mixture of **26e** (0.887 g, 4.23 mmol), **27k** (1 g, 4.23 mmol), and K_2CO_3 (1.168 g, 8.464 mmol) in CH_3CN (15 mL) was stirred at 80ºC overnight. The mixture was diluted with water and extracted with EtOAc. The organic layer was washed with brine, dried over anhydrous Na_2SO_4, and concentrated in vacuo. The crude was purified by flash column chromatography (silica gel, petroleum ether/EtOAc 20/1 to 1/1) to give **28** (1 g, 51%). LCMS: m/z 410 $[M + H]^+$, *t*R = 0.753 min.

(S)-**2-(N-BOC-1-(N-BOC-aminomethylbenzylamino)-1-(1,2,3,4-tetrahydroquinolin-1-yl)ethan-1-one (29).** A mixture of **28** (1 g, 2.44 mmol), di-^{t}butyl dicarbonate (0.559 g, 2.564 mmol), and Et_3N (0.494 g, 4.884 mmol) in CH_2Cl_2 (15 mL) was stirred at 50ºC overnight. The mixture was quenched with 5% citric acid (aqueous solution). The organic layer was washed with brine, dried over anhydrous Na_2SO_4, and concentrated in vacuo. The crude was purified by flash column chromatography (silica gel, petroleum ether/EtOAc 20/1 to 5/1) to give **29** (0.6 g, 47%). LCMS: m/z 510 $[M + H]^+$, *t*R = 1.248 min.

(S)-**2-(N-BOC-1-(N-mehtyl-N-BOC-aminomethylbenzylamino)-1-(1,2,3,4-tetrahydroquinolin-1-yl)ethan-1-one (30).** To a solution of **29** (0.6 g, 1.177 mmol) in THF (12 mL) stirred at 0ºC under Nitrogen atmosphere, NaH (0.096 g, 2.354 mmol) was portion wise added and stirred for 15 minutes. Then methyl iodine (0.2 g, 1.41 mmol) was dropwise added and the resulting mixture was stirred at room temperature for 16h. Then, water was carefully added. The organic layer was collected and washed with brine, dried over anhydrous Na_2SO_4, and concentrated in vacuo. The crude was purified by flash column chromatography (silica gel, petroleum ether/EtOAc 20/1 to 5/1) to give **30** (0.32 g, 51%). LCMS: m/z 524 $[M + H]^+$, *t*R = 1.11 min.

(S)-**2-(1-methylaminomethylbenzylamino)-1-(1,2,3,4-tetrahydroquinolin-1-yl)ethan-1-one (17).** A mixture of **30** (0.13 g, 0.248 mmol) in HCl 4N solution in 1,4-dioxane (15 mL) was stirred at room temperature for 2 hours. Then the mixture was concentrated in vacuo and the residue thus obtained was dissolved in CH_2Cl_2, washed $NaHCO_3$ (aqueous saturated solution) and brine, dried over anhydrous

Na_2SO_4, and concentrated in vacuo. The crude was purified by flash column chromatography (silica gel, MeOH in DCM, 0/100 to 10/90) to give **17** (0.090 g, 85%). LCMS: m/z 524 $[M + H]^+$, *t*R = 1.11 min. ^{1}H NMR (400 MHz, DMSO-d_6) δ 10.47 (br s, 1H), 9.66 (br s, 1H), 9.11 (br s, 1H), 7.31-7.85 (m, 5H), 7.30-7.00 (m, 4H), 4.82 (br s, 1H), 4.23.7 (m, 5H), 3.16 (s, 3H), 2.53-2.85 (m, 3H), 1.49-2.11 (m, 2H). LCMS: m/z 397 $[M + H]^+$, *t*R = 0.561 min.

(S)-**2-(1-aminomethylbenzyloxy)-1-(1,2,3,4-tetrahydroquinolin-1-yl)ethan-1-one (31a).** To a solution of (*S*)-**27l** (0.3 g, 2.187 mmol) in THF (15 mL) at 0 °C was added portionwise NaH (0.131 g, 3.28 mmol). After 10 min stirring, **26e** (0.550 g, 2.624 mmol) was added and the resulting mixture was gradually warmed to room temperature and stirred for 1 day. The mixture was diluted with water and extracted with EtOAc. The organic layer was washed with brine, dried over anhydrous Na_2SO_4, and concentrated in vacuo. The crude was purified by flash column chromatography (silica gel, MeOH in CH_2Cl_2, 0/100 to 100/0) to give **31a** as a colorless oil (0.412 g, 61%). ^{1}H NMR (300 MHz, $CDCl_3$) δ 7.42 – 7.23 (m, 5H), 7.22 – 6.98 (m, 3H), 4.51 – 4.31 (m, 1H), 4.26 (d, *J* = 14.0 Hz, 1H), 4.08 (d, *J* = 14.0 Hz, 1H), 3.88 – 3.61 (m, 2H), 3.02 – 2.79 (m, 2H), 2.70 (t, *J* = 6.6 Hz, 2H), 2.06 – 1.87 (m, 2H). LCMS: m/z 311 $[M + H]^+$, *t*R = 1.06 min.

(S)-**2-(1-aminomethyl-4-bromobenzyloxy)-1-(6-fluoro-1,2,3,4-tetrahydroquinolin-1-yl)ethan-1-one (31b).** Starting from **26e** (0.388 g, 1.7 mmol) and (*S*)-**27g** (0.307 mg, 1.42 mmol) and following the procedure described for **31a**, compound **31b** was obtained as a white solid (0.578 g, 100%).

(S)-**2-(1-N-(2-nitrophenylsulfonylaminomethylbenzyloxy)-1-(1,2,3,4-tetrahydroquinolin-1-yl)ethan-1-one (32a)**. 2-Nitro-N-mehtyl-phenylsulfonyl chloride (0.294 g, 1.32 mmol) was dissolved in CH_2Cl_2 (9 mL), and the solution was cooled to 0 °C. Diisopropylethylamine (0.329 mL, 1.991 mmol) and **31a** (0.412 g, 1.327 mmol) were added, and the resulting solution was gradually warmed to room temperature and stirred overnight. $NaHCO_3$ (aqueous saturated solution) was added and extracted with CH_2Cl_2. The combined organic layer was dried using Na_2SO_4, and the solvent was removed under reduced pressure. The residue thus obtained was purified by flash column chromatography (silica gel, EtOAc in Heptane, 0/100 to 100/0) to give **32a** as a colorless oil (0.554 g, 84%). ^{1}H NMR (300 MHz,

$CDCl_3$) δ 8.09 (dd, J = 5.9, 3.3 Hz, 1H), 7.81 (dd, J = 5.9, 3.4 Hz, 1H), 7.73 – 7.58 (m, 2H), 7.37 – 7.23 (m, 5H), 7.11 (dd, J = 9.7, 6.9 Hz, 4H), 4.60 (dd, J = 9.4, 2.9 Hz, 1H), 4.29 (d, J = 14.8 Hz, 1H), 4.00 (d, J = 14.8 Hz, 1H), 3.77 (s, 2H), 3.49 – 3.36 (m, 1H), 3.21 (dd, J = 16.1, 6.0 Hz, 1H), 2.71 (t, J = 6.6 Hz, 2H), 1.96 (q, J = 6.6 Hz, 2H). LCMS: m/z 496 $[M + H]^+$, tR = 1.6 min.

(S)-**2-(1-N-(2-nitrophenylsulfonylaminomethyl-4-bromobenzyloxy)-1-(6-fluoro-1,2,3,4-tetrahydroquinolin-1-yl)ethan-1-one (32b)**. Starting from **31b** (0.578 g, 1.42 mmol) and following the procedure described for **32a**, compound **32b** was obtained as a colourless oil (0.293 g, 35%). ^{1}H NMR (300 MHz, $CDCl_3$) δ 7.99-8.13 (m, 1H), 7.78-7.90 (m, 1H), 7.60-7.77 (m, 2H), 7.45 (d, J=8.25 Hz, 2H), 6.76-7.23 (m, 5H), 4.62 (dd, J=2.75, 8.80 Hz, 1H), 4.27 (br d, J=14.57 Hz, 1H), 4.14 (q, J=7.15 Hz, 2H), 3.98 (br d, J=14.57 Hz, 1H), 3.56-3.90 (m, 1H), 3.37-3.56 (m, 1H), 3.15-3.33 (m, 1H), 2.73 (br t, J=6.05 Hz, 2H), 1.97 (quin, J=6.70 Hz, 2H). LCMS: m/z 594 $[M + H]^+$, tR = 1.68 min.

(S)-**2-(1-N-(2-nitro-N-methyl-phenylsulfonylaminomethylbenzyloxy)-1-(1,2,3,4-tetrahydroquinolin-1-yl)ethan-1-one (34a)**. Compound **32a** (0.2 g, 0.404 mmol), Cs_2CO_3 (0.197 g, 0.605 mmol) and **33a** (0.032 mL, 0.525 mmol) were suspended in DMF (3 mL), The mixture was stirred at room temperature overnight. Then, water was added and extracted with EtOAc. The combined organic layer was dried using Na2SO4, and the solvent was removed under reduced pressure. The residue thus obtained was purified by flash column chromatography (silica gel, EtOAc in Heptane, 0/100 to 15/85) to give **34a** (0.203 g, 99%). ^{1}H NMR (300 MHz, $CDCl_3$) δ 7.98 (dd, J = 6.0, 3.2 Hz, 1H), 7.72 – 7.54 (m, 3H), 7.32 (d, J = 11.8 Hz, 6H), 7.22 – 7.00 (m, 3H), 4.77 (t, J = 6.3 Hz, 1H), 4.17 (d, J = 13.3 Hz, 1H), 4.03 (d, J = 13.3 Hz, 1H), 3.73 (t, J = 6.3 Hz, 2H), 3.49 (d, J = 6.2 Hz, 2H), 2.96 (s, 3H), 2.70 (t, J = 6.5 Hz, 2H), 1.94 (q, J = 6.6 Hz, 2H). LCMS: m/z 510 $[M + H]^+$, tR = 4.03 min.

(S)-**2-(1-N-(2-nitro-N-ethyl-phenylsulfonylaminomethylbenzyloxy)-1-(1,2,3,4-tetrahydroquinolin-1-yl)ethan-1-one (34b)**. Starting from **32a** (0.128 g, 0.258 mmol) and **33b** (0.027 mL, 0.336 mmol) and following the procedure described for **32a**, compound **34b** was obtained (0.098 g, 72%). ^{1}H NMR (300 MHz, $CDCl_3$) δ 8.09 – 8.00 (m, 1H), 7.66 – 7.54 (m, 2H), 7.32 (s, 5H), 7.11 (s, 3H), 4.73 (dd, J = 7.9,

4.5 Hz, 1H), 4.13 (d, *J* = 13.0 Hz, 1H), 3.98 (d, *J* = 13.2 Hz, 1H), 3.77 – 3.36 (m, 6H), 2.74 – 2.56 (m, 2H), 1.93 (p, *J* = 6.6 Hz, 2H), 1.09 (t, *J* = 7.1 Hz, 3H). LCMS: m/z 524 $[M + H]^+$, *t*R = 1.66 min.

***(S)*-2-(1-N-(2-nitro-N-ethyl-phenylsulfonylaminomethylbenzyloxy)-1-(1,2,3,4-tetrahydroquinolin-1-yl)ethan-1-one (34c)**. Starting from **32a** (0.224 g, 0.452 mmol) and **33c** (0.159 mL, 0.678 mmol) and following the procedure described for **34a**, compound **34c** was obtained (0.182 g, 70%). ^{1}H NMR (300 MHz, $CDCl_3$) δ 7.39 – 7.23 (m, 6H), 7.21 – 7.00 (m, 3H), 4.57 (dd, *J* = 9.0, 2.9 Hz, 1H), 4.26 (d, *J* = 14.3 Hz, 1H), 4.06 (d, *J* = 14.3 Hz, 1H), 3.73 (d, *J* = 6.3 Hz, 2H), 3.35 – 3.12 (m, 2H), 3.09 – 2.95 (m, 1H), 2.82 (dd, *J* = 12.6, 2.9 Hz, 1H), 2.69 (t, *J* = 6.6 Hz, 2H), 1.94 (q, 2H). LCMS: m/z 578 $[M + H]^+$, *t*R = 4.41 min.

***(S)*-2-(1-N-(2-nitro-N-ethyl-phenylsulfonylaminomethyl-4-bromobenzyloxy)-1-(6-fluoro-1,2,3,4-tetrahydroquinolin-1-yl)ethan-1-one (34d)**. Starting from **32b** (0.293 g, 0.495 mmol) and **33c** (0.173 mL, 0.742 mmol) and following the procedure described for **34a**, compound **34c** was obtained (0.255 g, 76%). LCMS: m/z 676 $[M + H]^+$, *t*R = 1.83 min.

***(S)*-2-(1-N-(2-nitro-N-ethyl-phenylsulfonylaminomethyl-4-pyridyl-benzyloxy)-1-(6-fluoro-1,2,3,4-tetrahydroquinolin-1-yl)ethan-1-one (34d)**. To a stirred suspension of **34d** (0.100g, 0.148 mmol), pyridinylboronic acid (0.024 g, 0.178 mmol) and Na_2CO_3 (0.031 g, 0.297 mmol) in 1,4-dioxane (5 mL) was added $PdCl_2(dppf)_2$ (0.006 g, 0.007 mmol) and the mixture was heated at 90 °C for 16h. The mixture was cooled to room temperature and filtered through a Celite pad. The filtrate was diluted with water (20 mL) and extracted with EtOAc (2 × 15 mL). The organic layer was washed with brine (15 mL), dried over anhydrous Na2SO4, and concentrated in vacuo. The crude was purified by flash column chromatography (silica; AcOEt in heptane 0/100 to 100/0) to give the desired product **34d** as a yellow solid (0.087 g, 87%). LCMS: m/z 673 $[M + H]^+$, *t*R = 1.54 min.

***(S)*-2-(1-ethylaminomethyl-4-pyridyl-benzyloxy)-1-(6-fluoro-1,2,3,4-tetrahydroquinolin-1-yl)ethan-1-one (22)**. LiOH (0.033, 0.776 mmol) and 2-mercaptoethanol (0.011 mL, 0.158 mmol) were added to a solution of **34d** (0.087 g, 0.129 mmol) in DMF (0.8 mL) stirred at 0ºC. Then, the resulting mixture was stirred at room temperature overnight. Then, water was added and extracted with EtOAc.

The combined organic layer was dried using Na_2SO_4, and the solvent was removed under reduced pressure. The residue thus obtained was purified by flash column chromatography (silica gel, MeOH in CH_2Cl_2, 0/100 to 15/85) to give **22** as colorless oil (0.036 g, 57%). ^{1}H NMR (300 MHz, $CDCl_3$) δ 8.69 (d, J=6.05 Hz, 2H), 7.65 (d, J=8.11 Hz, 2H), 7.36-7.56 (m, 4H), 6.71-6.96 (m, 3H), 5.32 (s, 1H), 4.67 (br d, J=6.46 Hz, 1H), 4.21-4.39 (m, 1H), 4.01-4.19 (m, 1H), 3.73 (br s, 2H), 3.29 (q, J=9.26 Hz, 2H), 3.01-3.19 (m, 1H), 2.89 (br d, J=12.51 Hz, 1H), 2.72 (br t, J=6.39 Hz, 2H), 1.97 (quin, J=6.56 Hz, 2H).

(S)-**2-(1-methylaminomethylbenzyloxy)-1-(1,2,3,4-tetrahydroquinolin-1-yl)ethan-1-one (18)**. Starting from **34a** (0.203 g, 0.398 mmol) and following the procedure described for **22**, compound **18** was obtained as colorless oil (0.054 g, 41%). ^{1}H NMR (300 MHz, DMSO-d_6) δ 7.23-7.61 (m, 6H), 6.91-7.20 (m, 3H), 4.52 (br dd, *J*=3.64, 8.18 Hz, 1H), 4.25 (d, *J*=14.16 Hz, 1H), 4.06 (d, *J*=14.16 Hz, 1H), 3.61 (tdd, *J*=6.36, 12.75, 19.21 Hz, 2H), 2.55-2.97 (m, 5H), 2.34 (s, 3H), 1.85 (quin, *J*=6.70 Hz, 2H) LCMS: m/z 325 $[M + H]^+$, *t*R = 2.07 min

(S)-**2-(1-dimethylaminomethylbenzylamino)-1-(1,2,3,4tetrahydroquinolin-1-yl)ethan-1-one (19)**. NaH (0.036 mg, 0.908 mmol) was added to a solution of (*S*)-**27h** (0.152 g, 0.726 mmol) in THF (4 mL) at 0ºC. The mixture was stirred for 10 min at 0ºC and NaH (0.086 mg, 2.14 mmol) was added portion wise. Then, **26e** (0.100 g, 0.614 mmol) was added and the resulting mixture was gradually warmed to room temperature and stirred for 16h. The mixture was diluted with water and extracted with EtOAc. The organic layer was washed with brine, dried over anhydrous Na_2SO_4, and concentrated in vacuo. The crude was purified by flash column chromatography (silica gel, MeOH in DCM, 0/100 to 10/90) to give **19** (0.083 g, 38%). ^{1}H NMR (300 MHz, DMSO-d_6) δ 7.43 (br s, 1H), 7.24-7.36 (m, 5H), 7.02-7.18 (m, 3H), 4.54 (br t, *J*=6.19 Hz, 1H), 4.15 (d, *J*=13.47 Hz, 1H), 4.04 (d, *J*=13.47 Hz, 1H), 3.54-3.70 (m, 2H), 2.57-2.74 (m, 3H), 2.30-2.47 (m, 1H), 2.17 (s, 6H), 1.77-1.95 (m, 2H). LCMS: m/z 339 $[M + H]^+$, *t*R = 2.31 min.

(S)-**2-(1-ethylaminomethylbenzyloxy)-1-(1,2,3,4-tetrahydroquinolin-1-yl)ethan-1-one (20)**. Starting from **34b** (0.098 g, 0.452 mmol) and following the procedure described for **22**, compound **20** was obtained (0.032 g, 43%). ^{1}H NMR (300 MHz, $CDCl_3$) δ 6.92-7.56 (m, 9H), 4.63 (dd, *J*=3.02, 9.07 Hz,

1H), 4.28 (d, *J*=14.16 Hz, 1H), 4.12 (d, *J*=14.16 Hz, 1H), 3.75 (dt, *J*=5.84, 12.41 Hz, 1H), 2.62-3.05 (m, 5H), 2.21 (br d, *J*=13.33 Hz, 3H), 1.84-2.07 (m, 2H), 1.18 (t, *J*=7.15 Hz, 3H). LCMS: m/z 339 $[M + H]^+$, *t*R = 2.12 min.

(S)-**2-(1-ethylaminomethylbenzyloxy)-1-(1,2,3,4-tetrahydroquinolin-1-yl)ethan-1-one (21)**. Starting from **34c** (0.182 g, 0.315 mmol) and following the procedure described for **22**, compound **21** was obtained (0.097 g, 77%). ^{1}H NMR (300 MHz, $CDCl_3$) δ 6.93-7.47 (m, 9H), 4.59 (dd, *J*=2.89, 9.07 Hz, 1H), 4.28 (d, *J*=14.30 Hz, 1H), 4.06 (d, *J*=11.13 Hz, 1H), 3.56-3.92 (m, 2H), 3.15-3.39 (m, 2H), 3.05 (dd, *J*=9.28, 12.44 Hz, 1H), 2.84 (dd, *J*=2.96, 12.58 Hz, 1H), 2.71 (t, *J*=6.60 Hz, 2H), 1.96 (quin, *J*=6.70 Hz, 3H). LCMS: m/z 393 $[M + H]^+$, *t*R = 2.47 min.

(S)-**2-(1-methylaminomethyl)-4-fluorobenzylamino)1-(1,2,3,4-tetrahydroquinolin-1-yl)ethan-1-one (23)**. Starting from **26e** (0.104 g, 0.497 mmol) and (*S*)-**27i** (0.070 g, 0.414 mmol) and following the procedure described for **19**, compound **23** was obtained (0.020 g, 14%). ^{1}H NMR (300 MHz, DMSO-d_6) δ 8.36 (br s, 1H), 6.93-7.80 (m, 7H), 4.80 (br d, *J*=8.25 Hz, 1H), 4.42 (br d, *J*=15.26 Hz, 1H), 4.15 (br d, *J*=15.40 Hz, 1H), 3.46-3.81 (m, 2H), 2.92-3.30 (m, 3H), 2.60-2.81 (m, 4H), 1.86 (quin, *J*=6.25 Hz, 2H). LCMS: m/z 343 $[M + H]^+$, *t*R = 2.35 min.

(S)-**2-(1-methylaminomethyl)-4-benzylamino)-1-(6-fluoro-1,2,3,4-tetrahydroquinolin-1-yl)ethan-1-one (24)**. Starting from **26f** (0.2 g, 0.88 mmol) and (*S*)-**27j** (0.120 g, 0.8 mmol) and following the procedure described for **19**, compound **24** (0.092 g, 33%). ^{1}H NMR (300 MHz, DMSO-d_6) δ 7.64 – 7.41 (m, 1H), 7.41 – 7.22 (m, 5H), 7.07 – 6.88 (m, 2H), 4.47 (s, 1H), 4.21 (d, *J* = 14.2 Hz, 1H), 4.04 (d, *J* = 14.0 Hz, 1H), 3.70 – 3.50 (m, 2H), 2.77 – 2.62 (m, 3H), 2.58 – 2.51 (m, 1H), 2.27 (s, 3H), 1.92 – 1.77 (m, 2H). LCMS: m/z 343 $[M + H]^+$, *t*R = 2.33 min.

(S)-**2-(1-methylaminomethyl)-4-fluorobenzylamino)-1-(6-fluoro-1,2,3,4-tetrahydroquinolin-1-yl)ethan-1-one (25)**. Starting from **26f** (0.21 g, 0.922 mmol) and (*S*)-**27i** (0.130 g, 0.768 mmol) and following the procedure described for **19**, compound **25** was obtained (0.070 g, 25%). ^{1}H NMR (300 MHz, $CDCl_3$) δ 6.25-8.10 (m, 7H), 4.80 (br d, *J*=9.49 Hz, 2H), 4.32 (br d, *J*=15.53 Hz, 1H), 4.06 (br s,

1H), 3.70 (br s, 2H), 3.25 (br d, *J*=12.23 Hz, 1H), 2.34-3.03 (m, 6H), 1.91 (br d, *J*=5.50 Hz, 2H). LCMS: m/z 361 $[M + H]^+$, *t*R = 2.401 min.

ASSOCIATED CONTENT

Supporting information

HPLC reports for the purity check of the target compounds and intermediates.

Author Information

*Corresponding Authors.

(J.M.C.) Tel.: +34 925 245750. E-mail: jcid@its.jnj.com

(A.A.T.) Tel.: +34 925 245750. E-mail: atrabanc@its.jnj.com

Author Contributions

J.M.C., G.T., H.L. and A.A.T. conceived the project and designed experiments. F.T., G.T., L.P.B., A.A.T. and A.F. performed experiments. J.M.C., G.T., L.P.B., H.L. and A.A.T. analyzed and interpreted results. J.M.C., G.T., H.L. and A.A.T. wrote and revised the manuscript.

Funding

This work was supported by Janssen R&D.

Notes

The authors declare no competing financial interest.

ACKNOWLEDGMENTS

The authors thank members of the purification and analysis group and the in vitro metabolism team from Janssen R&D.

References

[1] Bradley, S.-R., Levey, A.-I., Hersch, S.-M., and Conn, P.-J. (1996) Immunocytochemical localization of group III metabotropic glutamate receptors in the hippocampus with subtype-specific antibodies. *Neurosci. 16*, 2044-2056.
[2] Saugstad, J.-A., Kinzie, J.-M., Mulvihill, E.-R., Segerson, T.-P., and Westbrook, G.-L., (1993) Cloning and expression of a new member of the L-2-amino-4-phosphonobutyric acid-sensitive class of metabotropic glutamate receptors. *Mol. Pharmacol. 45*, 367-372.
[3] Corti, C., Restituito, S., Rimland, J.-M., Brabet, I., Corsi, M., Pin, J.-P., and Ferraguti, F. (1998) Cloning and characterization of alternative mRNA forms for the rat metabotropic glutamate receptors mGluR7 and mGluR8. *Eur. J. Neurosci. 10*, 3629-3641.
[4] Kinoshita, A., Shigemoto, R., Ohishi, H., van der, P.-H., and Mizuno, N. (1998) Immunohistochemical localization of metabotropic glutamate receptors, mGluR7a and mGluR7b, in the central nervous system of the adult rat and mouse: A light and electron microscopic study. *J. Comp. Neurol. 393*, 332-352.
[5] Kinzie, J.-M., Saugstad, J.-A., Westbrook, G.-L., and Segerson, T.-P. (1995) Distribution of metabotropic glutamate receptor 7 messenger RNA in the developing and adult rat brain. *Neuroscience 69*, 167-176.
[6] Ohishi, H., Nomura, S., Ding, Y.-Q., Shigemoto, R., Wada, E., Kinoshita, A., Li, J.-L., Neki, A., Nakanishi, S., and Mizuno, N. (1995) Presynaptic localization of a metabotropic glutamate receptor, mGluR7, in the primary afferent neurons: an immunohistochemical study in the rat. *Neurosci. Lett. 202*, 85-88.
[7] Bahi, A., Fizia, K., Dietz, M., Gasparini, F., and Flor, P.-J. (2012) Pharmacological modulation of mGluR7 with AMN082 and MMPIP exerts specific influences on alcohol consumption and preference in rats. *Addict Biol. 17*, 235−247.
[8] Fendt, M., Schmid, S., Thakker, D.-R., Jacobson, L.-H., Yamamoto, R., Mitsukawa, K., Maier, R., Natt, F., Husken, D., Kelly, P.-H., McAllister, K.-H., Hoyer, D., van der Putten, H., Cryan, J.-F., and Flor, P.-J. (2008) mGluR7 facilitates extinction of aversive memories and controls amygdala plasticity. *Mol. Psychiatry 13*, 970−979.
[9] Pelkey, K.-A., Yuan, X., Lavezzari, G., Roche, K.-W., and McBain, C.-J. (2007) mGluR7 undergoes rapid internalization in response to activation by the allosteric agonist AMN082. *Neuropharmacology 52*, 108−117.
[10] Wieronska, J.-M., Stachowicz, K., Acher, F., Lech, T., and Pilc, A. (2012) Opposing efficacy of group III mGlu receptor activators, LSP1- 2111 and AMN082, in animal models of positive symptoms of schizophrenia. *Psychopharmacology* (Berl) *220*, 481−494.
[11] Konieczny, J., and Lenda, T. (2013) Contribution of the mGluR7 receptor to antiparkinsonian-like effects in rats: a behavioral study with the selective agonist AMN082. *Pharmacol. Rep. 65*, 1194−1203.
[12] Bradley, S.-R., Uslaner, J.-M., Flick, R.-B., Lee, A., Groover, K.-M., and Hutson, P.-H. (2012) The mGluR7 allosteric agonist AMN082 produces antidepressant-like effects by modulating glutamatergic signaling. *Pharmacol., Biochem. Behav. 101*, 35−40.
[13] Dolan, S., Gunn, M.-D., Biddlestone, L., and Nolan, A.-M. (2009) The selective metabotropic glutamate receptor 7 allosteric agonist AMN082 inhibits inflammatory pain-induced and incision-induced hypersensitivity in rat. *Behav. Pharmacol. 20*, 596−604.
[14] Li, X., Li, J., Peng, X.-Q., Spiller, K., Gardner, E.-L., and Xi, Z.-X. (2009) Metabotropic glutamate receptor 7 modulates the rewarding effects of cocaine in rats: involvement of a ventral pallidal GABAergic mechanism. *Neuropsychopharmacology 34*:1783–1796.
[15] Li, X., Li, J., Gardner, E.-L., and Xi, Z.-X. (2010) Activation of mGluR7s inhibits cocaine-induced reinstatement of drug-seeking behavior by a nucleus accumbens glutamate-mGluR2/3 mechanism in rats. *J. Neurochem. 114*:1368–1380.
[16] Lavreysen, H., and Dautzenberg, F. M. (2008) Therapeutic potential of group III metabotropic glutamate receptors. *Curr. Med. Chem. 15*:671–684.
[17] Wright, R.-A., Arnold, M.-B., Wheeler, W.-J., Ornstein, P.-L., and Schoepp, D.-D. (2000) Binding of [^{3}H](2S,1′S,2′S)-2-(9-xanthylmethyl)- 2-(2′-carboxycyclopropyl) glycine ([3H]LY341495) to cell membranes expressing recombinant human group III metabotropic glutamate receptor subtypes. *Naunyn-Schmiedeberg's Arch. Pharmacol. 362*, 546−554.
[18] Wu, S., Wright, R.-A., Rockey, P.-K., Burgett, S.-G., Arnold, J.-S., Rosteck, P.-R., Jr., Johnson, B.-G., Schoepp, D.-D., and Belagaje, R. M. (1998) Group III human metabotropic glutamate receptors 4, 7 and 8: molecular cloning, functional expression, and comparison of pharmacological properties in RGT cells. *Brain Res. Mol. Brain Res. 53*, 88−97.
[19] Makoff, A., Pilling, C., Harrington, K., and Emson, P. (1996) Human metabotropic glutamate receptor type 7: molecular cloning and mRNA distribution in the CNS. *Brain Res. Mol. Brain Res. 40*, 165−170.
[20] Cryan, J.-F., Kelly, P.-H., Neijt, H.-C., Sansig, G., Flor, P.-J., and van der Putten, H. (2003) Antidepressant and anxiolytic-like effects in mice lacking the group III metabotropic glutamate receptor mGluR7. *Eur. J. Neurosci. 17*, 2409-2417.
[21] Callaerts-Vegh, Z., Beckers, T., Ball, S.-M., Baeyens, F., Callaerts, P.-F., Cryan, J.-F., Molnar, E. and D'Hooge, R. (2006) Concomitant deficits in working memory and fear extinction are functionally dissociated from reduced anxiety in metabotropic glutamate receptor 7-deficient mice. *J. Neurosci.*, *26*, 6573-6582.
[22] Niswender, C. M., and Conn, P. J. (2010) Metabotropic glutamate receptors: physiology, pharmacology, and disease. *Annu. Rev. Pharmacol. Toxicol 50*, 295−322.
[23] Hamilton, S. P. (2011) A new lead from genetic studies in depressed siblings: assessing studies of chromosome 3. *Am. J. Psychiatry 168*, 783-789.

[24] Breen, G., Webb, B. T., Butler, A. W., van den Oord, E. J., Tozzi, F., Craddock, N., Gill, M., Korszun, A., Maier, W., Middleton, L., Mors, O., Owen, M. J., Cohen-Woods, S., Perry, J., Galwey, N. W., Upmanyu, R., Craig, I., Lewis, C. M., Ng, M., Brewster, S., Preisig, M., Rietschel, M., Jones, L., Knight, J., Rice, J., Muglia, P., Farmer, A. E., and McGuffin, P. (2011) A genome-wide significant linkage for severe depression on chromosome 3: the depression network study. *Am. J. Psychiatry 168*, 840−847.
[25] Ganda, C., Schwab, S.-G., Amir, N., Heriani, H., Irmansyah, I., Kusumawardhani, A., Nasrun, M., Widyawati, I., Maier, W., and Wildenauer, D.-B. (2009) A family-based association study of DNA sequence variants in GRM7 with schizophrenia in an Indonesian population. *Int. J. Neuropsychopharmacol. 12*, 1283−1289.
[26] Mick, E., Neale, B., Middleton, F.-A., McGough, J.-J., and Faraone, S.-V. (2008) Genome-wide association study of response to methylphenidate in 187 children with attention-deficit/hyperactivity disorder. *Am. J. Med. Genet., Part B 147B*: 1412−1418.
[27] Lindsley, C.-W., Emmitte, K.-A., Hopkins, C.-R., Bridges, T.-M., Gregory, K.-J., Niswender, C.-M., and Conn, P.-J. (2016) Practical Strategies and Concepts in GPCR Allosteric Modulator Discovery: Recent Advances with Metabotropic Glutamate Receptors *Chem. Rev. 116*, 6707-6741.
[28] Schoepp, D.-D., Jane, D.-E., and Monn, J.-A. (1999) Pharmacological agents acting at subtypes of metabotropic glutamate receptors. *Neuropharmacology 38*:1431–1476.
[29] Récasens, M., Guiramand, J., Aimar, R., Abdulkarim, A., and Barbanel, G. (2007) Metabotropic glutamate receptors as drug targets. *Curr. Drug Targets 8*, 651–681.
[30] Selvam, C., Goudet, C., Oueslati, N., Pin J.-P., and Acher, F.-C. (2007) l-(+)-2-Amino-4-thiophosphonobutyric acid (l-thioAP4), a new potent agonist of group III metabotropic glutamate receptors: increased distal acidity affords enhanced potency. *J. Med. Chem. 50*, 4656-4664.
[31] May, L.-T., Leach, K., Sexton, P.-M., and Christopoulos, A. (2007) Allosteric modulation of G protein-coupled receptors. *Annu. Rev. Pharmacol. Toxicol. 47*, 1–51.
[32] Bridges, T.-M., and Lindsley, C.-W. (2008) G-Protein-coupled receptors: from classical modes of modulation to allosteric mechanisms. *ACS Chem. Biol. 3*, 530–541.
[33] Christopoulos, A., Changeux, J.-P., Catterall, W. A., Fabbro, D., Burris, T. P., Cidlowski, J. A., Olsen, R. W., Peters, J. A., Neubig, R. R., Pin, J.-P., Sexton, P. M., Kenakin, T. P., Ehlert, F. J., Spedding, M., and Langmead, C. J. (2014) International union of basic and clinical pharmacology. XC. Multisite pharmacology: recommendations for the nomenclature of receptor allosterism and allosteric ligands. *Pharmacol. Rev. 66*, 918–947.
[34] Mitsukawa, K., Yamamoto, R., Ofner, S., Nozulak, J., Pescott, O., Lukic, S., Stoehr, N., Mombereau, C., Kuhn, R., McAllister, K., van der Putten, H., Cryan, J., and Flor, P. (2005) A selective metabotropic glutamate receptor 7 agonist: activation of receptor signaling via an allosteric site modulates stress parameters in vivo. *Proc. Natl. Acad. Sci. U.S.A. 102*, 18712-18717.
[35] Selvam, C., Oueslati, N., Lemasson, I.-A., Brabet, I., Rigault, D., Courtiol, T., Cesarini, S., Triballeau, N., Bertrand, H.-O., Goudet, C., Pin, J.-P., and Acher, F. (2010) A virtual screening hit reveals new possibilities for developing group III metabotropic glutamate receptor agonists. *J. Med. Chem. 53*, 2797–2813.
[36] Sukoff Rizzo, S.-J., Leonard, S.-K., Gilbert, A., Dollings, P., Smith, D.-L., Zhang, M.-Y., Di, L., Platt, B.-J., Neal, S., Dwyer, J.-M., Bender, C.-N., Zhang, J., Lock, T., Kowal, D., Kramer, A., Randall, A., Huselton, C., Vishwanathan, K., Tse, S. Y., Butera, J., Ring, R.-H., Rosenzweig-Lipson, S., Hughes, Z.-A., and Dunlop, J. (2011) The metabotropic glutamate receptor 7 allosteric modulator AMN082: a monoaminergic agent in disguise? *J. Pharmacol. Exp. Ther. 338*, 345−352.
[37] Jalan-Sakrikar, N., Field, J.-R., Klar, R., Mattmann, M.-E., Gregory, K.-J., Zamorano, R., Engers, D.-W., Bollinger, S.-R., Weaver, C.-D., Days, E.-L., Lewis, L.-M., Utley, T.-J., Hurtado, M., Rigault, D., Acher, F., Walker, A.-G., Melancon, B.-J., Wood, M.-R., Lindsley, C.-W., Conn, P.-J., Xiang, Z., Hopkins, C.-R., and Niswender, C.-M., (2014) Identification of positive allosteric modulators VU0155094 (ML397) and VU0422288 (ML396) reveals new insights into the biology of metabotropic glutamate receptor 7 *ACS Chem. Neurosci. 5*, 1221−1237.
[38] Abe, M., Seto, M., Gogliotti, R.-C., Loch, M.-T., Bollinger, K.-A., Chang, S., Engelberg, E.-M., Luscombe, V.-B., Harp, J.-M., Bubser, M., Engers, D.-W., Jones, C.-K., Rodriguez, A.-L., Blobaum, A.-L., Conn, J.-P., Niswender, C.-M., and Lindsley, C.-W. (2017) Discovery of VU6005649, a CNS penetrant $mGlu_{7/8}$ receptor PAM derived from a series of pyrazolo[1,5-a]pyrimidines. *ACS Med. Chem. Lett. 8*, 1110-1115.
[39] Tresadern, G., Trabanco, A.-A., Pérez-Benito, L., Overington, J.-P., Van Vlijmen, H.-W., and van Westen, G.-J. (2017) Identification of allosteric modulators of metabotropic glutamate 7 receptor using proteochemometric modeling. *J. Chem. Inf. Model.57*, 2976–2985.
[40] Flor, P.-J., Marzinzik, A., Nozulak, J., Ofner, S., Roy, B., and Spanka, C., (2007) Preparation of substituted diamines as mGluR7 regulators. WO 2007025709 A2.
[41] Farinha, A., Lavreysen, H., Peeters, L., Russo, B., Masure, S., Trabanco, A., Cid, J., and Tresadern, G., (2015) Molecular determinants of positive allosteric modulation of the human metabotropic glutamate receptor 2. *Br. J. Pharmacol. 172*, 2383-2396.

[42] Doornbos, M.-L.-J., Pérez-Benito, L., Tresadern, G., Mulder-Krieger, T., Biesmans, I., Trabanco, A.-A., Cid, J.-M., Lavreysen, H., IJzerman, A.-P., and Heitman, L.-H., Molecular mechanism of positive allosteric modulation of the metabotropic glutamate receptor 2 by JNJ-46281222. (2016) *Br. J. Pharmacol. 173*, 588-600.
[43] Cid, J.-M., Tresadern, G., Vega, J.-A., de Lucas, A.-I., del Cerro, A., Matesanz, E., Linares, M.-L., García, A., Iturrino, L., and Pérez-Benito, L., Macdonald, G.-J., Oehlrich, D., Lavreysen, H., Peeters, L., Ceusters, M., Ahnaou, A., Drinkenburg, W., Mackie, C., Somers, M., and Trabanco, A.-A., (2016) Discovery of 8-trifluoromethyl-3-cyclopropylmethyl-7-[(4-(2, 4-difluorophenyl)-1-piperazinyl) methyl]-1, 2, 4-triazolo [4, 3-a] pyridine (JNJ-46356479), a selective and orally bioavailable mGlu2 receptor positive allosteric modulator (PAM). *J. Med. Chem. 59*, 8495-8507.
[44] Pérez-Benito, L., Doornbos, M.-L.-J., Cordomí, A., Peeters, L., Lavreysen, H., Pardo, L., and Tresadern, G., (2017) Molecular switches of allosteric modulation of the metabotropic glutamate 2 receptor. *Structure 25*, 1153-1162.
[45] Sansuk, K., Deupi, X., Torrecillas, I.-R., Jongejan, A., Nijmeijer, S., Bakker, R.-A., Pardo, L., and Leurs, R.-A., (2011) Structural insight into the reorientation of transmembrane domains 3 and 5 during family A G protein-coupled receptor activation. *Mol. Pharmacol. 79*, 262-269.
[46] Venkatakrishnan, A.-J., Deupi, X., Lebon, G., Tate, C.-G., Schertler, G.-F., and Babu, M.-M. Molecular signatures of G-protein-coupled receptors. *Nature 494*, 185-194.
[47] Doré, A.-S., Okrasa, K., Patel, J.-C., Serrano-Vega, M., Bennett, K., Cooke, R.-M., Errey, J.-C., Jazayeri, A., Khan, S., and Tehan, B., (2014) Structure of class C GPCR metabotropic glutamate receptor 5 transmembrane domain. *Nature 511*, 557-562.
[48] Wu, H., Wang, C., Gregory, K.-J., Han, G.-W., Cho, H.-P., Xia, Y., Niswender, C.-M., Katritch, V., Meiler, J., Cherezov, V., Conn, P. J., Stevens, R. C. (2014) Structure of a class C GPCR metabotropic glutamate receptor 1 bound to an allosteric modulator. *Science 344*, 58–64.
[49] Rasmussen, S.-G.-F., DeVree, B.-T., Zou, Y., Kruse, A.-C., Chung, K.-Y., Kobilka, T.-S., Thian, F.-S., Chae, P.-S., Pardon, E., and Calinski, D. (2011) Crystal Structure of the β2 adrenergic receptor–Gs protein complex. *Nature 477*, 549–555.
[50] Suzuki, G., Tsukamoto, N., Fushiki, H., Kawagishi, A., Nakamura, M., Kurihara, H., Mitsuya, M., Ohkubo, M. and Ohta, H. (2007) In Vitro Pharmacological Characterization of Novel Isoxazolopyridone Derivatives as Allosteric Metabotropic Glutamate Receptor 7 Antagonists. *J. Pharmacol. Exp. Ther.*, 323 (1) 147-156.

Table of Contents Graphic

Computationally Guided Identification of Allosteric Agonists of the Metabotropic Glutamate 7 Receptor

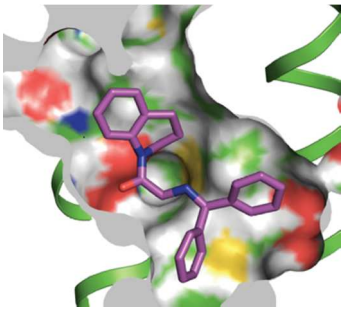

Docked binding mode of an Allosteric Agonists of the mGlu7 receptor at the 7TM domain.